Composites: Part B 69 (2015) 94–100

Contents lists available at ScienceDirect

Composites: Part B

journal homepage: www.elsevier.com/locate/compositesb

Mechanical and thermal properties of carbon fiber/polypropylene composite filled with nano-clay

Mohamed H. Gabr [a,b,*], Wataru Okumura [c], Hisai Ueda [c], Wataru Kuriyama [c], Kiyoshi Uzawa [a], Isao Kimpara [a]

[a] Laboratory for Integrated Technological Systems, Kanazawa Institute of Technology, 924-0838, Japan
[b] Faculty of Industrial Education, Sohag University, 611111, Egypt
[c] Industrial Research Institute of Ishikawa, 920-8203, Japan

ARTICLE INFO

Article history:
Received 7 March 2014
Received in revised form 19 June 2014
Accepted 24 September 2014
Available online 2 October 2014

Keywords:
A. Carbon fiber
B. Fracture toughness
B. Thermal properties
A. Thermoplastic resin

ABSTRACT

The effect of organoclay on the mechanical and thermal properties of woven carbon fiber (CF)/compatibilized polypropylene (PPc) composites is investigated. Polypropylene–organoclay hybrids nanocomposites were prepared using a maleic anhydride-modified PP oligomer (PP-g-MA) as a compatibilizer. Different weight percentages of Nanomer® I-30E nanoclay were dispersed in PP/PP-g-MA (PPc) using a melt mixing method. The PPc/organoclay nanocomposite was then used to manufacture plain woven CF/PPc nanocomposites using molding compression process. CF/PPc/organoclay composites were characterized by different techniques, namely; dynamic mechanical analysis (DMA), fracture toughness and scanning electron microscope. The results revealed that at filler content 3% of organoclay, initiation and propagation interlaminar fracture toughness in mode I were improved significantly by 64% and 67% respectively, which could be explained by SEM at given weight as well; SEM images showed that in front of the tip, fibers pull out during initiation delamination accounting for fracture toughness improvement. Dynamic mechanical analysis showed enhancement in thermomechanical properties. With addition 3 wt.% of organoclay, the glass transition temperature increased by about 6 °C compared to neat CF/PPc composite indicating better heat resistance with addition of organoclay.

1. Introduction

There are increasing interests in using thermoplastics to replace thermosets for laminate fabrication due to their advantages such as high toughness, shorter manufacturing cycles, no refrigeration storage required and reprocessing possibilities [1]. Carbon fiber or glass fiber reinforced thermoplastic laminates in matrices such as polyetherimide (PEI), polyetheretherketone (PEEK) and polyphenylene sulfide (PPS) have already been used extensively in the aerospace sector due to their excellent mechanical properties, heat stability and low flammability [2,3]. These matrices are, however, expensive and difficult to process due to the high processing temperature and pressure.

Among the available thermoplastic polymers, polypropylene (PP) is considered a good candidate as thermoplastic composite matrix. Polypropylene is a semi-crystalline engineering thermoplastic and is known for its balance of strength, modulus and chemical resistance [4]. Polypropylene has many potential applications in automobiles, appliances and other commercial products in which creep resistance, stiffness and some toughness are demanded in addition to weight and cost savings. However, the CFRP fabrication from neat PP resin cannot meet the industrial requirements due to its low mechanical properties especially toughness and low thermal resistance. To improve the strength and thermal properties of CF composites, various types of nano-filler (such as clay, silica, graphene, and CNT) have been incorporated into the thermosets and thermoplastics matrices. The incorporation of inorganic particulate as well as fiber fillers has been proved to be an effective way to improving the physical and thermal properties [5–18].

Nanoclay, an inexpensive natural mineral, has been reported by many studies as one of the potential candidates for nanocomposite and CFRP preparations because of its large value of aspect ratio, diameter in nanometer range and thermal resistivity [19,20]. In most cases, in order to provide a better physical and chemical environment for the polymer, clay is organically modified through an ion exchange reaction between organic cations and inorganic cations,

* Corresponding author at: Laboratory for Integrated Technological Systems, Kanazawa Institute of Technology, 924-0838, Japan. Tel.: +81 762748269.
E-mail address: mgabr@neptune.kanazawa-it.ac.jp (M.H. Gabr).

http://dx.doi.org/10.1016/j.compositesb.2014.09.033
1359-8368/

to change the clay from hydrophilic to organophilic and to increase interlayer spacing of clay [21].

Polypropylene–clay based nanocomposites are of tremendous research interest due to the improved properties with low clay content as well as the clay serving as a valuable cost effective additive. In general, 0–5 wt.% of organically treated clay is added in PP polymer matrix. The addition of the nanoclay in the PP matrix increases the thermal stability in air medium, increases physical properties (dimensional stability), improves flame retardant properties (increased thermal-oxidative stability and reduced Heat Release Rate), improves mechanical properties, fracture properties and gas barrier properties. Several studies were conducted with various types of organoclays, clay concentrations and compatibilizers [22–24,10].

To the best of our knowledge, the effect of organoclay on the mechanical properties of CF/PPc composites has not been studied yet. In the present study, thermal and mechanical behavior of CF/PPc composites filled with organoclay were investigated. Polypropylene–organoclay hybrids nanocomposites were prepared using a maleic anhydride-modified PP oligomer (PP-g-MA) as a compatibilizer. Different weight percentages of Nanomer® I-30E nanoclay, a surface modified montmorillonite mineral, were dispersed in PP/PP-g-MA (PPc) using melt mixing method. The PPc/clay nanocomposites were then used to manufacture plain weave carbon/PP nanocomposites using molding compression process. CF/PPc/organoclay composites were characterized by different techniques, namely; bending, dynamic mechanical analysis (DMA), fracture toughness, and scanning electron microscope. Also, PPc/organoclay nanocomposites were characterized by X-ray diffraction (XRD), Differential Scanning Calorimeter (DSC), and tensile tests.

2. Experimental

2.1. Materials

Polypropylene (Novatec SA08 containing 1% MA-g-PP with MFR 75 g/10 min) was purchased from Polypropylene Japan Co., Montmorillonite clay (Nanomer® I.30E, a surface modified montmorillonite mineral) containing 25–30 wt.% octadecylamine with bulk density 200–500 kg/m^3 was purchased from sigma Aldrich Japan.

2.2. Preparation of PPc/organoclay nanocomposite and CFRP laminates

PPc and organoclay were dry blended prior to melt-blending on a twin-screw extruder until the mixture was evenly mixed. The mixture was then taken out and molded into sheets of 0.1 mm thickness by a hot press at 180°C and 3 MPa for 5 min using a hydraulic hot press machine, then, cooled to room temperature at the same pressure. The sheets were prepared for structure and mechanical characterization. The PPc/organoclay nanocomposites were then used to manufacture plain weave carbon/PP nanocomposites using molding compression process.

Carbon fiber laminates were manufactured by stacking the pre-impregnated carbon fabric with the fabricated PPc/organoclay attending the reinforcement/matrix volume fraction of 52/48 ± 2 (v/v).

2.3. Hot compression molding

The composite laminate consolidation process using the compression molding was carried out in a steel mold with dimensions of 200 × 220 mm. Firstly, the composite laminate was heated up to 200 °C at 10 °C/min, holding at this temperature for 10 min. Afterwards, the composite laminate was cooled down to the desired compressing temperature of 160 °C at 10 °C/min and consolidated under 15 MPa of pressure. The mold was cooled to room temperature by cooling system. Fig. 1 shows the heating cycle process.

2.4. Characterization

2.4.1. X-ray diffraction (XRD)

The structure of the nanocomposites was studied by using XRD. A Philips PW1050 diffractometer was used to obtain the X-ray diffraction patterns using Cu Kα lines (λ = 1.5406 Å). The diffractrograms were scanned from 2.1° to 35° (2θ) using a scanning rate of 2°/min. X-ray diffractrograms were taken on organoclay particles and on PPc/organoclay nanocomposites.

2.4.2. Differentials scanning calorimeter (DSC)

A DSC-2910 apparatus made by TA Instrument Inc. (USA) was used for investigating crystallization process of PPc and PPc/organoclay nanocomposites. All measurements were carried out in room temperature. Ten milligrams of the polymer sample was weighed very accurately in the aluminum DSC pan and placed in the DSC cell. The sample was heated from room temperature to 200 °C. The sample was cooled to 30 °C at a constant rate of 10 °C/min, and the heat flow curve was recorded as a function of temperature.

2.4.3. Tensile tests of PPc/organoclay nanocomposites

The tensile tests for PPc/organoclay nanocomposites were carried out using Universal Testing Machine (Shimadzu, AG-X) at a crosshead speed of 1 mm/min with gauge length 50 mm at room temperature according to ASTM D-638. Five samples of each category were tested and their average values were reported.

2.4.4. Dynamic mechanical analysis of CF/PPc/organoclay nanocomposites

RSAIII instrument was used to perform the DMA studies in order to evaluate the storage modulus and tan δ. The CFRP laminates samples with dimensions 50 mm long × 6.5 mm wide × 2 mm thick were tested in three-point bending at varying temperatures between −45 °C and 200 °C at a heating rate of 3 °C/min and a frequency of 1.0 Hz. The glass transition temperatures, T_g, of nanocomposites were also determined from the maxima of the tan δ curves.

2.4.5. Fracture toughness test of CF/PPc/organoclay nanocomposites

The double cantilever beam (DCB) mode I fracture specimen (ASTM D 5528-01) was employed to characterize the delamination resistance of CFRP laminates. The corrections for the end-block,

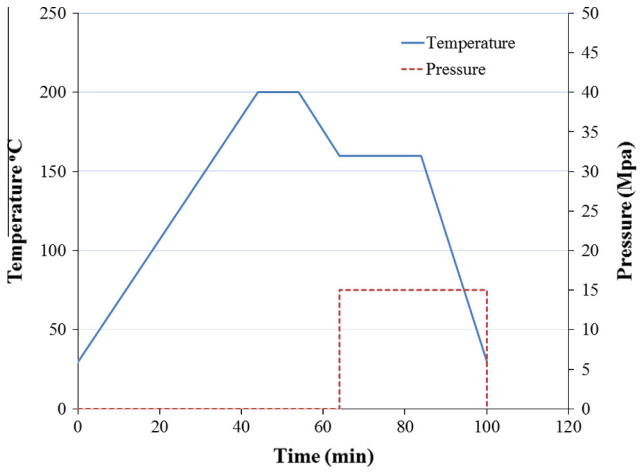

Fig. 1. Heating cycle used in the hot molding compression for PP/CF/organoclay composites.

DCB arm bending and root rotation were considered. DCB tests were conducted using a universal mechanical testing machine. The recommended specimen size is at least 150 mm long and 20 mm wide with an initial crack length (i.e. the length of the insert from the load line) of 50 mm (see Fig. 2). Hinges of the same width as the specimen were attached to allow load application. The mode-I interlaminar fracture toughness G_{IC} and G_{IP}, for each organoclay content was calculated using the modified beam theory (MBT) calculated from Eq. (1):

$$G_{IC} = \frac{3P_c(\delta_c/N)}{2B(a+\Delta)}F \qquad G_{IP} = \frac{3P_p(\delta_p/N)}{2B(a+\Delta)}F \tag{1}$$

where G_{IC} is fracture toughness at initial crack stage, G_{IP} is fracture toughness at propagation stage, P_p is the applied load, δ_p is displacement, a is crack length, P_c is the initial maximum load, δ_c the corresponding initial displacement, B is specimen width, Δ is crack length correction factor (determined from the least square plots of cubic root of compliance, $C^{1/3}$, against the crack length), N is end-block correction factor.

2.4.6. Scanning electron microscopy observations

Fractured surfaces obtained from fracture toughness tests were examined by scanning electron microscopy (SEM) using JSM-7001FD equipment. Prior to SEM observation, all samples were sputter coated with a thin layer of gold to avoid electrical charging.

3. Results

3.1. Structure of PPc–clay nanocomposites

The structure and morphology of nanoclay filled PPc composites was examined using XRD method. Fig. 3 shows the XRD patterns of PPc–organoclay series. The organonanoclay shows a diffraction peak of 2θ at 4.12° and corresponds to an interlayer spacing of nanoclay (d-spacing) of 21.13 Å (calculated from Bragg's diffraction law of $2d\sin\theta = n\lambda$). At 1 wt.% of organoclay in the PPc polymer, there is an absence of a diffraction peak, and this suggests that the matrix polymer has entered into the interlayer spacing of the organoclay and increased the original organoclay spacing above the level of 7.5 nm (in which Bragg's law cannot satisfy), or the nanolayers of organoclays could have randomly dispersed in the PPc polymer. Hence, it can be concluded that the organoclays in the PPc polymer at 1 wt.% formed an ordered exfoliated structure, or a randomly dispersed clay exfoliated structure.

At 3 and 5 wt.% organoclay onwards, there exists a diffraction peak in the composite specimens. At 3 wt.% organoclay, the organoclay diffraction peak shifted to a lower 2θ value of 2.33° and this corresponds to an interlayer of organoclay of 38.06 Å. At 5 wt.% organoclay, the diffraction peak occurs at a 2θ value of 2.38° and corresponds to the interlayer spacing of organoclays of

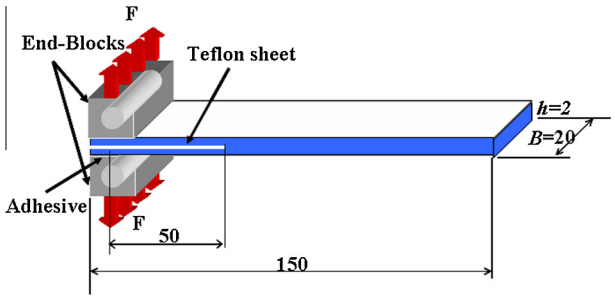

Fig. 2. Geometry of DCB specimen (all dimensions in mm).

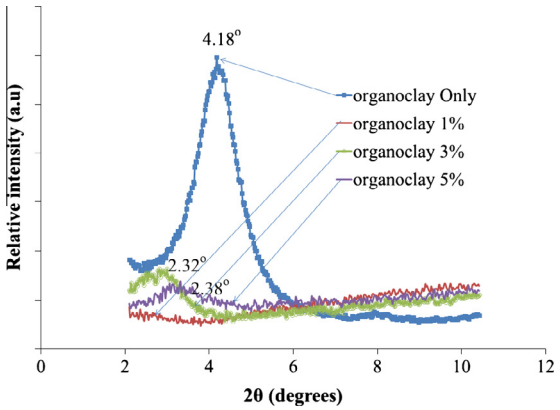

Fig. 3. XRD pattern at 2.1–10.5° of compatibilized PPc/organoclay composite.

37.10 Å. XRD results for 3 wt.% and 5 wt.% organoclay shows that the composites formed intercalated nanocomposites structures.

3.2. Crystallization and melting behaviors of PPc nanocomposites

Fig. 4 shows the DSC cooling curves of neat PPc and PPc/organoclay nanocomposites with organoclay loading up to 5 wt.%. The crystallization peak temperature of PPc is 121.1 °C, while 5 wt.% organoclay addition increases this temperature up to 123.4 °C. The DSC cooling curves clearly show that the addition of a small amount of organoclay into the PP matrix results in an increase of crystallization temperature of the polymer matrix. This could be explained by the assumption that the organoclay layers act as efficient nucleating agents for the crystallization of the PP matrix. There is powerful interaction between PP molecules and the layers of organoclay, so the layers of organoclay can easily adsorb the PP molecules segments and some PP molecules are immobilized. These immobilized molecules of PP contribute to the crystallization process of PP; therefore the crystallization of PP molecules can occur at a higher temperature. Some similar results have been reported by Mingliang and Demin [21].

Fig. 5 shows the DSC heating curves of PPc and PPc/organoclay nanocomposites. According to Fig. 5, the melt process of polymer is revealed. The result suggests that the melt peak temperatures of PPc and PPc/organoclay nanocomposites are similar, at 165 °C. The shape of the DSC heating curves of PPc and the PPc/organoclay nanocomposites are similar indicating that the addition of organoclay does not affect the melt process and the melt temperature of PPc.

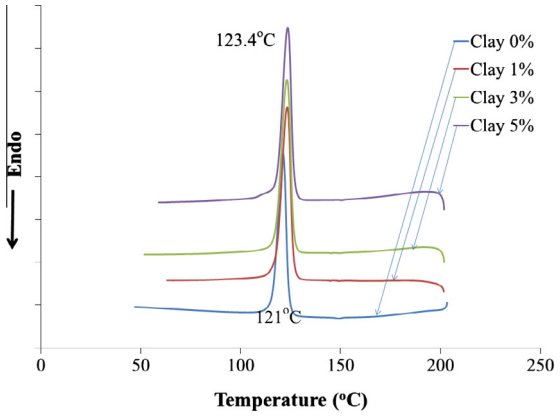

Fig. 4. Cooling curves of DSC for compatibilized PP/organoclay nanocomposites.

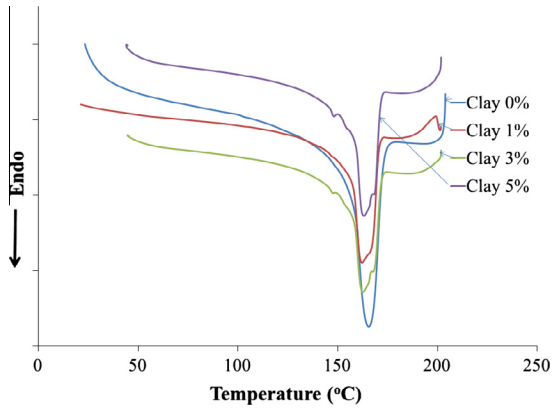

Fig. 5. Heating curves of DSC for compatibilized PP/organoclay nanocomposites.

3.3. Tensile properties for PPc nanocomposites

Tensile properties of nanocomposites and neat PPc were evaluated for reinforcing benefits of organoclay in polymer matrix (Fig. 6). It is revealed that the nanocomposites showed an improved tensile strength (17%, and 15% increment) compared to the neat PPc for 1%, and 3% nanomer loading respectively. Modulus of elasticity showed an improvement by about (61%, 130%, and 133% increment) compared to the neat PPc for 1%, 3% and 5% nanomer loading respectively. These improved tensile strength and modulus of compatibilized nanocomposites might be due to the conformational effects on the polymer at the polymer–organoclay interface. Addition of compatibilizer facilitates expansion of the gallery space of reinforcing nanolayers by inclusion of some polar groups (MA) to intercalate between the silicate layers through hydrogen bonding to the oxygen groups of silicate tetrahedra, resulting in an enhanced interlayer distance of stacked nanolayers, which in turn are separated nanolayers and dispersed homogeneously [23]. The miscibility of the maleated PP with polar groups of the nanoparticles and the PP matrix mediate between the surface chemistry of the polymer and the clay at the interphase, which contribute significantly to the increment in the strength as observed for other compatibilized systems [25,26]. However, the strength and values are lowered for 5% clay loading in comparison to neat PPc. The decreased strength for higher organoclay content is attributed to the increased amount of low molecular weight oligomer fraction of the maleated polypropylene.

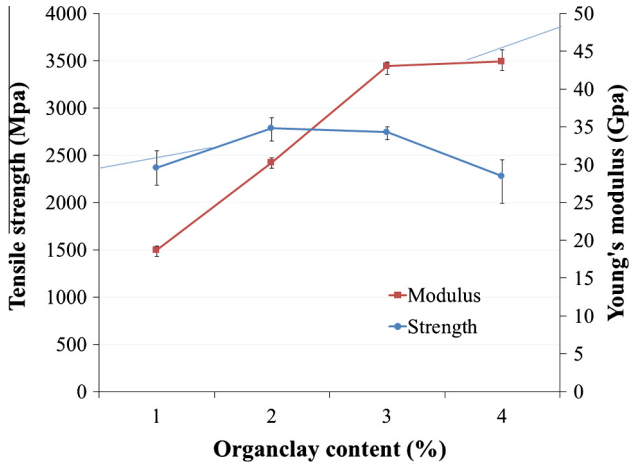

Fig. 6. Tensile strength and modulus for compatibilized PP/organoclay nanocomposites.

3.4. Dynamic mechanical behaviors of CFRP laminates

The effect of the incorporation of organoclay into CF/PPc on the thermal mechanical behavior of the composite material was investigated with DMA at the organoclay contents of 0, 1, 3, and 5 wt.% based on PP. Figs. 7 and 8 show the DMA data for CF/PPc composite with varying amounts of organoclay. One can recognize that the incorporation of organoclay results in increasing storage modulus in the whole temperature range above T_g, compared to the neat PPc. The storage moduli of PPc/CF composites increase with increasing organoclay loading up to 3.0 wt.% loading of organoclay, while further increasing of organoclay loadings leads to a slight reduction in the modulus in the whole range of temperature. As the organoclay loading is 3.0 wt.%, the storage modulus reaches the maximum value (46.9 GPa) below T_g, while reaches the maximum for 1 wt.% (46.3 GPa) above T_g which is ~17% higher than that of neat PPc (39.8 GPa). This can well be explained by the reinforcing effect of the nanoparticles leading to increased stiffness of CF/PPc composites.

Fig. 8 shows the evolution of the loss factor, $\tan\delta$ as the function of temperature. The neat CF/PPc shows a peak at 6 °C, corresponding to its glass transition temperature which was equal to the values for other systems [27,28]. The addition of organoclay shifts the $\tan\delta$ peak to a higher temperature and increase the magnitude of the $\tan\delta$ peak. With addition 3 wt.% of organoclay, the $\tan\delta$ shifts to 12.4 °C. As previously reported [29], clay/nanocomposites systems also did exhibit significant changes in glass transition temperature when clay was added to the PP/nanocomposites. The increase in T_g may be attributed to a loss in the mobility of chain segments of PPc resulting from the nanoparticle/matrix interaction. Impeded chain mobility is possible if the nanoparticles are well dispersed in the matrix. The particle surface-to-surface distances ('matrix bridges') should then be relatively small and chain segment movement may be restricted. Good adhesion of nanoparticles with the surrounding polymer matrix would additionally benefit the dynamic modulus by hindering molecular motion to some extent.

3.5. Fracture toughness properties

Double cantilever beam (DCB) tests were performed and the mode I interlaminar fracture toughness, GIc was determined. The typical load displacement curves recorded during the interlaminar fracture tests for CF/PPc composites filled with organoclay contents are shown in Fig. 9. The load increased linearly until it reached the maximum where the crack initiated, which is followed by a gradual decrease as the crack further propagated. There were characteristic stick-slips in all cases due to the variations in local

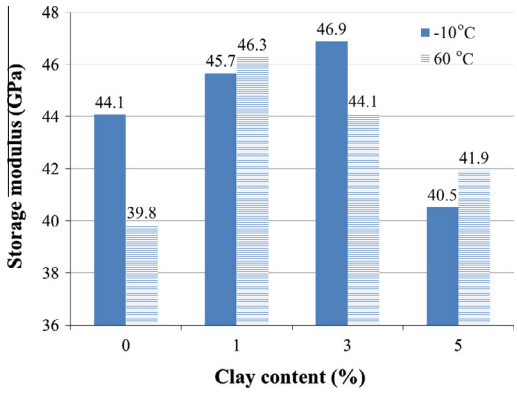

Fig. 7. Storage modulus at −10 and 60 °C for CF/PPc/organoclay nanocomposites.

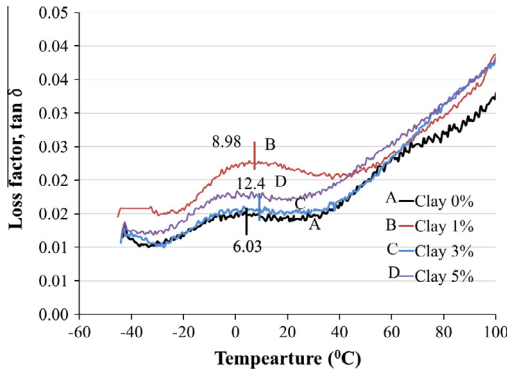

Fig. 8. tanδ and glass transition temperature for CF/PPc/organoclay nanocomposites.

material properties, such as resin-rich or fiber-rich regions along the longitudinal direction, misalignment of the fibers and voids, as well as the fracture of bridged fibers or fiber bundles [30]. The composites containing organoclay in the PPc exhibited higher load during extensions at complete fracture than those with neat PPc matrix (Fig. 9), suggesting higher resistance for crack growth behavior for the former composites.

The delamination resistance curves (*R*-curves) are drawn between crack length (a) and the corresponding fracture toughness as shown in Fig. 10. The GIc value corresponding to first crack initiation is determined from the load point at which the initiation of delamination is microscopically observed on the specimen edge. High deviations are noted for all fabric composites, probably as a consequence of the complex translaminar crack growth mechanism acting in the material. It has been observed that the crack growth rate of neat CF/PPc propagates smoothly as a result of the relatively low tenacity of the polymeric phase with carbon fiber; on the other hand, the crack of filled composites is deflected and pinned by the reinforcing obstacles so that more energy is required, resulting in higher fracture toughness.

Both delamination initiation and delamination propagation mode I fracture toughness values are plotted in Fig. 11. The delamination initiation mode I fracture toughness values reported throughout this investigation correspond to the first peak load in the load–crack opening displacement curves, while the delamination propagation mode I fracture toughness values are taken from the plateau region of the *R*-curves [31,32]. Various reasons such as intra-laminar delamination, fiber-bridging, micro-cracking, residual stresses, or a combination of these effects of lamina at interface caused the development of transverse intralaminar and unstable crack propagation in DCB tests [33]. In general, a number of mechanisms contribute to the fracture toughness and it is often very difficult to determine the dominant mechanism [34]. With organoclay addition those toughening mechanisms related to the layers silicate begin to act, which result in more superficial area and consequently larger fracture energy. The experimental GIc and GIp results obtained from MBT method for different ratios of organoclay are shown in Fig. 11. Both the initiation and propagation GIc values increased in general with increasing the organoclay concentration. This observation is consistent with previous reports [35] for unidirectional carbon fiber epoxy composites in that the initiation values of mode I interlaminar fracture toughness increased gradually with increasing clay contents. As shown in Fig.11. It is clear that fracture delamination resistance was improved significantly with addition organoclay up to 3 wt.%, the initial fracture toughness was increased significantly by about 64% from 145.8 J/m^2 for neat composite to 239.8 J/m^2 for 3 wt.% organoclay filled CF/PPc. The propagate fracture toughness for the same content was increased by about 67% from 151.7 J/m^2 for neat composites to 254.2 J/m^2. A less significant increase was observed for the initial fracture toughness at 5 wt.% organoclay,

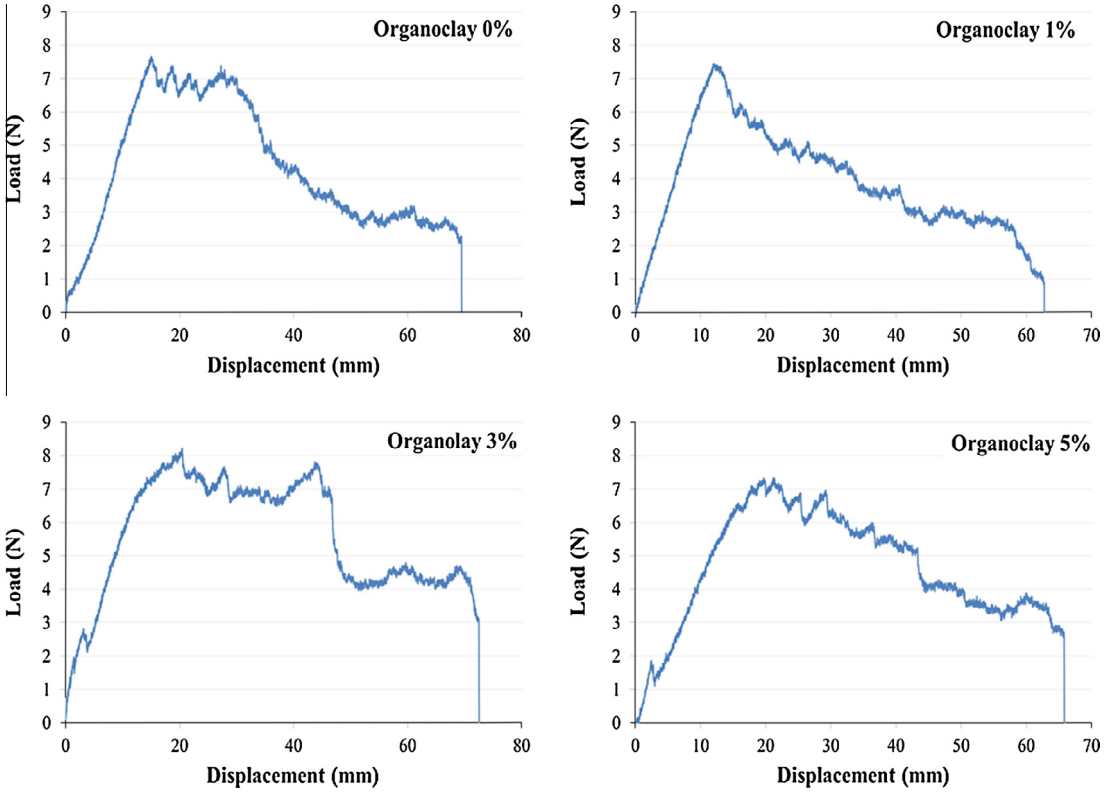

Fig. 9. Force–displacement curves for CF/PPc/organoclay nanocomposites.

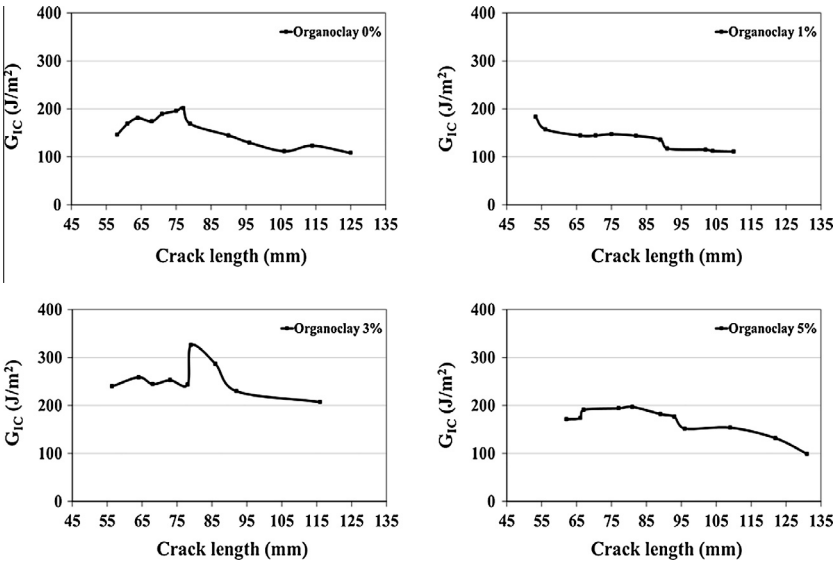

Fig. 10. *R*-curves for CF/PPc/organoclay nanocomposites.

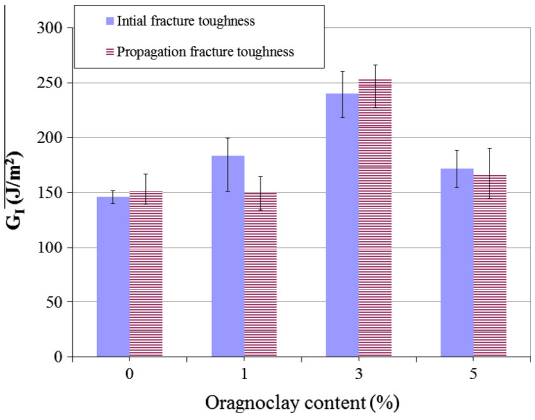

Fig. 11. Initial and propagation delamination for CF/PPc/organoclay nanocomposites.

the initial fracture toughness increased by about 17% from 145.8 J/m^2 for neat CF/PPc composite to 171.3 J/m^2, the propagate fracture toughness for the same content was increased by about 9% from 151.7 J/m^2 for neat CF/PPc composite to 165.6 J/m^2.

With reference to the fracture surface morphologies shown in Fig. 12, several important mechanisms are identified, which were responsible for the improved interlaminar fracture resistance in the CFRP composites containing organoclays. The micrograph for unfilled CF/PPc (Fig. 12a), shows a stepwise topography at the end of the insert film and fiber/matrix interface debonding. Apparently, large areas are covered by the PPc resin indicative of the reduction in delamination resistance. The hybrid CFRP composite samples containing organoclay in the matrix typically presented rougher matrix surface than those with neat PPc, resulting from the pinning and crack tip bifurcation, as discussed above (Fig. 12(b)–(d)). Two distinct regions exist in Fig 12(c) showing micrograph of CF/PPc filled 3 wt.% organoclay which exhibits the

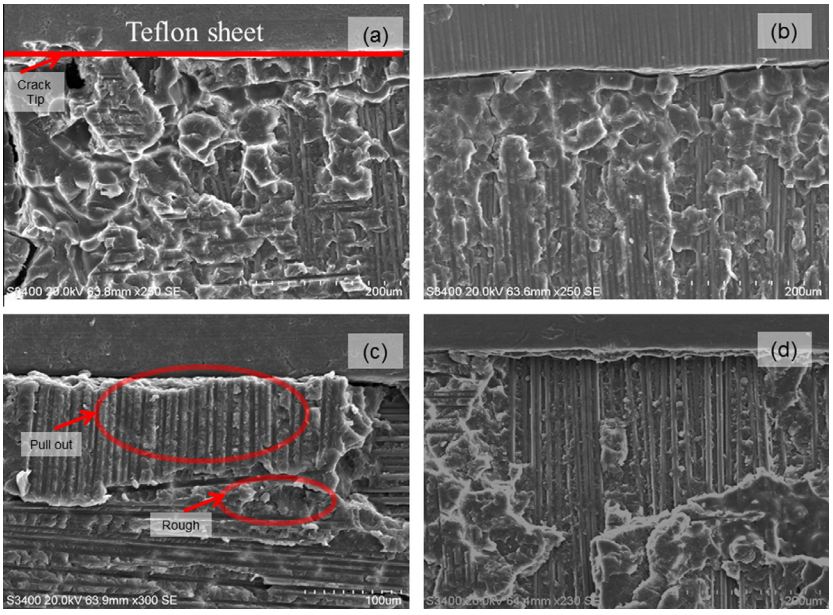

Fig. 12. SEM images for CF/PPc composites filled with different ratios of organoclay at fracture surface of fracture toughness testing specimens; (a) unfilled, (b) 1%, (c) 3%, and (d) 5% organoclay.

highest value of fracture toughness: the first is the rough region showing reinforced adhesion, while the second one, at the front of the tip of film insert, some fibers can be seen pulled out or broken without matrix coating. The rough areas of the CFRP suggest a strong bond exists at the interface between the CF and PP as a result of the strengthening effect resulting from the dispersed nanoparticles. In front of the tip, fibers pull out was taken place during the initiation delamination which could be resulted from fiber–polymer interaction, and fiber–fiber interaction. Fiber–polymer interaction promoted a large number of carbon fiber to break at the fracture surfaces resulting in consuming substantial fracture energy. While the rough area and matrix deformation between fibers became more extensive and deeper at high clay concentrations (Fig. 12d), there were only marginal increases in quasi-static fracture toughness, because the organoclay agglomerates tended to become larger in size with increasing the clay content. If the agglomerate sizes are unnecessarily large, they could be fractured more easily without providing effective barrier for pinning and bifurcation of the advancing cracks. The implication of this observation is that a low content of clay already led to a large improvement in quasi-static fracture toughness of nanocomposites and higher clay contents did not help further improvements.

4. Conclusion

In this study, we focused our attention to studying the effect of organoclay on the interfacial adhesion between plain woven carbon fiber (CF) and compatibilized polypropylene. The work concentrated on the experimental determination of the dynamic mechanical and fracture toughness properties of the CF/PPc/organoclay composite. The results reveal that a given weight of organoclay content of 3 wt.% plays a major role to improve initiation and propagation interlaminar fracture toughness in mode I significantly by about 64% and 67% respectively. The enhanced fracture toughness of the CF/PPc composites is attributable to the reinforcing effects of nanoclay. The SEM micrographs indicated relatively rough areas were formed confirming a high delamination resistance. The glass transition temperature increased by about 6 °C for 3 wt.% organoclay compared to neat CF/PPc composite indicating better heat resistance with addition of organoclay.

Acknowledgments

This work is a part of the Ishikawa Carbon Fiber Cluster Project supported by Regional Innovation Strategy Support Program (The Ministry of Education, Culture, Sports, Science and Technology (MEXT)).

References

[1] Shen Zhiqi, Bateman Stuart, Wu Dong Yang, McMahon Patrick, Olio Mel Dell, Gotama Januar. The effects of carbon nanotubes on mechanical and thermal properties of woven glass fibre reinforced polyamide-6 nanocomposites. Compos Sci Technol 2009;69:239–44.
[2] Diaz J, Rubio L. Development to manufacture structural aeronautical parts in carbon fibre reinforced thermoplastic materials. J Mater Process Technol 2003;143–144:342–6.
[3] Parlevliet Patricia P, Bersee Harald EN, Beukers Adriaan. Residual stresses in thermoplastic composites – a study of the literature – Part I: Formation of residual stresses. Compos A Appl Sci Manuf 2006;37(11):1847–57.
[4] Jeencham Rachasit, Suppakarn Nitinat, Jarukumjorn Kasama. Effect of flame retardants on flame retardant, mechanical, and thermal properties of sisal fiber/polypropylene composites. Composites Part B 2014;56:249–53.
[5] Phong NT, Gabr MH, Anh LH, Duc VM, Betti A, Okubo K, et al. Improved fracture toughness and fatigue life of carbon fiber reinforced epoxy composite due to incorporation of rubber nanoparticles. J Mater Sci 2013;48(17):6039–47.
[6] Phong NT, Gabr MH, Okubo K, Chuong B, Fujii T. Enhancement of mechanical properties of carbon fabric/epoxy composites using micro/nano-sized bamboo fibrils. Mater Des 2013;47:624–32.
[7] Gardea Frank, Lagoudas Dimitris C. Characterization of electrical and thermal properties of carbon nanotube/epoxy composites. Composites Part B 2014;56:611–20.
[8] Shiu Sung-Chiun, Tsai Jia-Lin. Characterizing thermal and mechanical properties of graphene/epoxy nanocomposites. Composites Part B 2014;56:691–7.
[9] Phong NT, Gabr MH, Okubo K, Chuong B, Fujii T. Improvement in the mechanical performances of carbon fiber/epoxy composite with addition of nano-(polyvinyl alcohol) fibers. Compos Struct 2013;99:380–7.
[10] Gabr Mohamed H, Phong Nguyen T, Abdelkareem Mohammad Ali, Okubo Kazuya, Uzawa Kiyoshi, Kimpara Isao, et al. Mechanical, thermal, and moisture absorption properties of nano-clay reinforced nano-cellulose biocomposites. Cellulose 2013;20(2):819–26.
[11] Gabr Mohamed H, Okubo Kazuya, Abd Elrahman Mostafa, Fujii Toru. Effect of microfibrillated cellulose on mechanical properties of plain woven CFRP reinforced epoxy. Compos Struct 2010;92(9):1999–2006.
[12] Jiang Qian, Wang Xin, Zhu Yuntian, Hui David, Qiu Yiping. Mechanical, electrical and thermal properties of aligned carbon nanotube/polyimide composites. Composites Part B 2014;56:408–12.
[13] GABR Mohamed H, Abdelrahman Mostafa, Okubo Kazuya, Fujii Toru. Interfacial adhesion improvement of plain woven carbon fibre reinforced epoxy filled with micro-fibrillated cellulose by addition liquid rubber. J Mater Sci 2010;45:3841–50.
[14] Barakat Nasser AM, Kim Bongsoo, Yi Chuan, Jo Younghun, Jung Myung-Hwa, Chu Kong Hee, Kim Hak Yong. Influence of cobalt nanoparticles' incorporation on the magnetic properties of the nickel nanofibers: cobalt-doped nickel nanofibers prepared by electrospinning. J Phys Chem C 2009;113:19452–7.
[15] Mohamed HGABR, Phong NguyenT, Kazuya OKUBO, Uzawa Kiyoshi, Kimpara Isao, Toru FUJII. Thermal and mechanical properties of electrospun nano-cellulose reinforced epoxy nanocomposites. Polym Testing 2014;37:51–8.
[16] Takagi Hitoshi, Nakagaito AN, Bistamam MSA. Extraction of cellulose nanofiber from waste papers and application to reinforcement in biodegradable composites. J Reinf Plast Compos 2013;32(20):1542–6.
[17] GABR Mohamed H, Abdelrahman Mostafa, Okubo Kazuya, Fujii Toru. A study on mechanical properties of bacterial cellulose/epoxy reinforced by plain woven carbon fiber modified with liquid rubber. J Compos A 2010;41:1263–71.
[18] Chen Qi, Weidong Wu, Zhao Yong, Xi Min, Tao Xu, et al. Nano-epoxy resins containing electrospun carbon nanofibers and the resulting hybrid multi-scale composites. Composites Part B 2014;58:43–53.
[19] Nopphawan Phonthammachai, Xu Li, Siewyee Wong, Hongling Chia, Weng Weei Tjiu, Chaobin He. Fabrication of CFRP from high performance clay/epoxy nanocomposite: preparation conditions, thermal–mechanical properties and interlaminar fracture characteristics. Composites Part A 2011;42:881–7.
[20] Pandey Jitendra Kumar, Singh Raj Pal. Green nanocomposites from renewable resources: effect of plasticizer on the structure and material properties of clay-filled starch. Starch 2005;57(1):8–15.
[21] mingliang Ge, demin Jia. Preparation and properties of polypropylene/clay nanocomposites using an organoclay modified through solid state method. J Reinf Plast Compos 2009;28:5–16.
[22] Ramsaroop A, Kanny K, Mohan TP. Fracture toughness studies of polypropylene–clay nanocomposites and glass fibre reinforced polypropylene composites. Mater Sci Appl 2010;1:301–9.
[23] Suin Supratim, Maiti Sandip, Shrivastava Nilesh K, Khatua BB. Mechanically improved and optically transparent polycarbonate/clay nanocomposites using phosphonium modified organoclay. Mater Des 2014;54:553–63.
[24] Shokrieh Mahmood M, Kefayati Amir R, Chitsazzadeh Majid. Fabrication and mechanical properties of clay/epoxy nanocomposite and its polymer concrete. Mater Des 2012;40:443–52.
[25] Parija S, Nayak SK, Verma SK, Tripathy SS. Studies on physico-mechanical properties and thermal characteristics of polypropylene/layered silicate nanocomposites. Polym Compos 2004;25(6):646–52.
[26] Lee Joong-Hee, Jung Daeseung, Hong Chang-Eui, Rhee Kyong Y, Advani Suresh G. Properties of polyethylene-layered silicate nanocomposites prepared by melt intercalation with a PP-g-MA compatibilizer. Compos Sci Technol 2005;65:1996–2002.
[27] Harismendy, Miner R, Valea A, Llano-Ponte R, Mujika F, Mondragon I. Strain rate and temperature effects on the mechanical behaviour of epoxy mixtures with different crosslink densities. Polymer 1997;38:5573.
[28] Charlesworth JM. Effect of crosslink density on molecular relaxations in diepoxide–diamine network polymers. Part 2. The rubbery plateau region. Polym Eng Sci 1988;28(4):230–6.
[29] Wetzel Bernd, Haupert Frank, Zhang Ming Qiu. Epoxy nanocomposites with high mechanical and tribological performance. Compos Sci Technol 2003;63:2055–67.
[30] Kim JK, Mai YW. High strength, high fracture toughness fibre composites with interface control—a review. Compos Sci Technol 1991;41:333–78.
[31] Velmurugan R, Solaimurugan S. Improvements in mode I interlaminar fracture toughness and in-plane mechanical properties of stitched glass/polyester composites. Compos Sci Technol 2007;67(1):61–9.
[32] Shah Khan MZ, Mouritz AP. Fatigue behaviour of stitched GRP laminates. Compos Sci Technol 1996;56(6):695–701.
[33] Ray D, Sarkar BK, Bose NR. Impact fatigue behaviour of vinylester resin matrix composites reinforced with alkali treated jute fibers. Compos A Appl Sci Manuf 2002;33(2):233–41.
[34] Silva RV, Spinelli D, Bose Filho WW, Claro Neto S, Chierice GO, Tarpan JR. Fracture toughness of natural fibers/castor oil polyurethane composites. Compos Sci Technol 2006;66(10):1328–35.
[35] Becker O, Varley RJ, Simon JP. Use of layered silicates to supplementarily toughen high performance epoxy–carbon fiber composites. J Mater Sci Lett 2003;22:1411–4.